TECHNICAL NOTES

NATIONAL ADVISORY COMMITTEE FOR AERONAUTICS

No. 542

THE INITIAL TORSIONAL STIFFNESS OF SHELLS WITH INTERIOR WEBS

By Paul Kuhn
Langley Memorial Aeronautical Laboratory

Washington
September 1935

NATIONAL ADVISORY COMMITTEE FOR AERONAUTICS

TECHNICAL NOTE NO. 542

THE INITIAL TORSIONAL STIFFNESS OF SHELLS WITH INTERIOR WEBS

By Paul Kuhn

SUMMARY

A method of calculating the stresses and torsional stiffnesses of thin shells with interior webs is summarized. Comparisons between experimental and calculated results are given for 3 duralumin beams, 5 stainless steel beams, and 2 duralumin wings. It is concluded that if the theoretical stiffness is multiplied by a correction factor of 0.9, experimental values may be expected to check calculated values within about 10 percent.

INTRODUCTION

It is well known that the application of ordinary engineering formulas to thin sheet-metal structures may lead to serious errors in some cases. For certain types of calculations, however, standard formulas will give a reasonable degree of accuracy if experimentally determined correction factors are applied. In the present paper U.S. Army Air Corps data on the tests of wings of the central box type are analyzed and the correction factor for initial torsional stiffness is derived. Since the methods of calculating torsion tubes with interior walls are not very widely known, the first part of the paper gives a summary of a convenient method elucidated by a numerical example. The second part of the paper discusses the most important features of the test objects and results.

LIST OF SYMBOLS

- T, torque, in.-lb.
- f_s, shearing stress, lb. per sq.in.
- t, thickness, in.
- ds, differential element of perimeter, in.
- A, area bounded by median line, sq.in.
- J, torsion constant, analogous to moment of inertia in bending, $in.^4$
- G, modulus of shear, lb. per sq.in.
- GJ, torsional stiffness, $lb.-in.^2$
- θ, angle of twist, radians (per unit length).
- η, factor of effectiveness in torsional stiffness.

I. THEORETICAL FORMULAS

General remarks.- The fundamental torsion formulas for thin shells such as shown in figure 1 are

$$f_s = \frac{T}{2At} \qquad (1)$$

$$J = \frac{4A^2}{\int \frac{ds}{t}} \qquad (2)$$

the integral being taken around the perimeter of the profile. The derivation and the assumptions underlying these formulas may be found in any good textbook on strength of materials, such as reference 1.

The corresponding formulas for shells with longitudinal interior webs (fig. 2) are not so well known as the fundamental formulas. Their derivation by different methods may be found in references 2 to 5, of which 2 and 5 are most readily available. The present paper will confine itself to showing how the torsional stresses and stiffnesses of such shells may be calculated. The method presented here is that given in reference 4 and was chosen because it permits the shortest possible exposition of the subject. The method given in references 2 and 5 is very similar; reference 3 gives a method based on the membrane analogy (reference 1). The most elaborate discussion of the physical foundations of the theory is given in reference 5.

Method of calculation.- The interior webs will divide the cross section of the shell into a number of separate cells. Numbers from one to n are assigned to these cells; the number zero is assigned to the space outside of the shell. The wall and anything pertaining to it between the two cells i and j are designated by the subscript ij. For each cell i is now computed the area A_i and for each wall ij the line integral

$$a_{ij} = \int \frac{ds}{t} \tag{3}$$

An auxiliary function F is now introduced for each cell i except cell zero, and the equation

$$T = 2 \sum_{i=1}^{i=n} F_i A_i \tag{4}$$

and n equations of the form

$$\frac{1}{A_i} \Sigma (F_j - F_i) a_{ij} + 2G\theta = 0 \tag{5}$$

may be written down. The summation in equation (5) extends over all walls bounding the cell i, i.e., for j are substituted in turn all numbers between zero and n that designate the cells surrounding cell i.

The system of equations (4) and (5) is solved for the unknowns $G\theta$ and F_i. The shearing stress in the wall ij is then given by

$$f_{s_{ij}} \doteq \frac{F_j - F_i}{t_{ij}} \tag{6}$$

The direction ij is positive if a point traveling along the wall keeps cell i on its left. In figure 3 the positive directions are indicated by arrows. It is evident that

$$f_{s_{ij}} = -f_{s_{ji}} \tag{7}$$

The torsion constant follows from

$$J = \frac{T}{G\theta} \tag{8}$$

The equations (4) and (5) applied to the three-cell system of figure 2 are

$$T = 2\left[A_1 F_1 + A_2 F_2 + A_3 F_3\right] \tag{4a}$$

$$\left.\begin{aligned}
&\frac{1}{A_1}\left[-a_{10}F_1 + a_{12}(F_2 - F_1)\right] + 2G\theta = 0 \\
&\frac{1}{A_2}\left[-a_{20}F_2 + a_{21}(F_1 - F_2) + a_{23}(F_3 - F_2)\right] + 2G\theta = 0 \\
&\frac{1}{A_3}\left[-a_{30}F_3 + a_{32}(F_2 - F_3)\right] + 2G\theta = 0
\end{aligned}\right\} \tag{5a}$$

For a shell with only one interior web (fig. 3), the values of F_i and J can be obtained directly from

$$\left.\begin{aligned}
F_1 &= \frac{1}{2}\,\frac{a_{20}A_1 + a_{12}A}{a_{20}A_1^{\,2} + a_{12}A^2 + a_{01}A_2^{\,2}}\,T \\
F_2 &= \frac{1}{2}\,\frac{a_{01}A_2 + a_{12}A}{a_{20}A_1^{\,2} + a_{12}A^2 + a_{01}A_2^{\,2}}\,T \\
J &= 4\,\frac{a_{20}A_1^{\,2} + a_{12}A^2 + a_{01}A_2^{\,2}}{a_{01}a_{12} + a_{12}a_{20} + a_{20}a_{01}}
\end{aligned}\right\} \tag{9}$$

where $A = A_1 + A_2$

For more than one interior web the formulas become too cumbersome, and it is more convenient to write down the equations (4) and (5) after the coefficients have been obtained and to solve these numerical equations.

The method discussed can be used for analyzing a shell such as shown in figure 4 where the cover sheet is provided with closed longitudinal stiffeners. Consider first the case in which the top and bottom sheets are of the same thickness and all stiffeners are of the same size (fig. 4(a)). As indicated on the figure by dotting all but one of the n stiffeners, only one stiffener need be considered because all functions will be the same for all stiffeners. Instead of obtaining a system of $(n + 1)$ equations of the type (5), only the following three equations appear:

$$\left.\begin{aligned} T &= 2\left[F_1 A_1 + nF_2 A_2\right] \\ \frac{1}{A_1}\left[-a_{10}F_1 + na_{12}(F_2 - F_1)\right] &+ 2G\theta = 0 \\ \frac{1}{A_2}\left[-a_{20}F_2 + a_{21}(F_1 - F_2)\right] &+ 2G\theta = 0 \end{aligned}\right\} \quad (10)$$

where $A_1 = A - nA_2$, A denoting the area bounded by the outer shell and A_2 the area under one stiffener; the line integrals a_{20} and a_{12} are taken for one stiffener.

In the more usual case where the top and bottom covers have different thicknesses and stiffeners, the equations become

$$\left.\begin{aligned} T &= 2\left[F_1 A_1 + nF_2 A_2 + mF_3 A_3\right] \\ \frac{1}{A_1}\left[-a_{10}F_1 + na_{12}(F_2 - F_1) + ma_{13}(F_3 - F_1)\right] &+ 2G\theta = 0 \\ \frac{1}{A_2}\left[-a_{20}F_2 + a_{21}(F_1 - F_2)\right] &+ 2G\theta = 0 \\ \frac{1}{A_3}\left[-a_{30}F_3 + a_{31}(F_1 - F_3)\right] &+ 2G\theta = 0 \end{aligned}\right\} \quad (11)$$

In these equations, the cell number 1 refers to the main part of the shell, number 2 to the area under a top stiffener (as in fig. 4(a)), and 3 to the area under a bottom stiffener; there are n top stiffeners and m bottom stiffeners.

When computing the line integral a_i for a stiffener, it is conservative to use the full developed length and unconservative to use the developed length between rivets. If the average of the two lengths is used, the error in J should be very small because stiffeners contribute normally only little to the total torsional stiffness.

The equations for the case of figure 4(a) may be obtained in a slightly different manner that is, perhaps, a little more physically obvious. Since the stress conditions are equal and uniform along the top and bottom surfaces, the stiffness of the shell is obviously not changed if all the stiffeners are transferred to one side and combined into a continuous corrugated sheet (fig. 4(b)). All rivet rows except the outer two may now be removed and the shell is reduced to a shell with a single interior web for the purpose of computing the initial stiffness. Naturally, such a relocation of stiffeners would change the stiffness under large torques as well as the strength.

Approximate method for stiffened cover.- The calculation of the torsional stiffness by the method described requires, in some cases, more time than is warranted considering the probable magnitude of the discrepancies between calculations and tests and considering the purpose of the calculation. In all cases where only an estimate of the torsional stiffness is required, and possibly in other cases, it will be sufficiently accurate to use the following approximate method for shells with stiffened cover.

Find the centroid of a single stiffener (without skin attached to it) and join the centroids of all stiffeners on one cover sheet by a line.

Along the line thus established, distribute the "effective" material of all stiffeners. The effective material of one stiffener is the actual material multiplied by the ratio $\frac{s_1}{s_2}$ (fig. 5).

There are now two separate sheets: the actual cover sheet and the "substitute stiffener sheet." Replace the two by a single sheet located at the centroid of the two and with a thickness equal to the sum of the two thicknesses.

The fundamental formula (1) can now be used to calculate the stiffness.

The results obtained by this approximate method will approach those obtained with the more exact method as the amount of material in the stiffeners becomes smaller in relation to the amount of material in the cover sheet and also as the ratio $\frac{s_1}{s_2}$ decreases. For the simple beams discussed in part II, the approximate results for the stiffness were from 2 to 8 percent higher than those from the exact method.

Numerical example.- As a numerical example of the general case, the stiffness calculation for the schematic profile of figure 6 will be given. With

$A_1 = 89.3 \qquad A_2 = 250 \qquad A_3 = 125$

$a_{10} = 514.4 \qquad a_{20} = 1875 \qquad a_{30} = 5190$

$a_{12} = 166.7 \qquad a_{23} = 333.3$

the equations become

$$T = 2\,(89.3\,F_1 + 250\,F_2 + 125\,F_3)$$

$$\frac{1}{89.3}\left[-514.4\,F_1 + 166.7\,(F_2 - F_1)\right] + 2G\theta = 0$$

$$\frac{1}{250}\left[-1875\,F_2 + 166.7(F_1 - F_2) + 333.3(F_3 - F_2)\right] + 2G\theta = 0$$

$$\frac{1}{125}\left[-5190\,F_3 + 333.3\,(F_2 - F_3)\right] + 2G\theta = 0$$

The results are

$$F_1 = 0.001667\ T$$

$$F_2 = 0.001254\ T$$

$$F_3 = 0.000310\ T$$

$$2G\theta = 0.01036\ T$$

Substitution of these values in equations (6) and (8) gives the shear stresses indicated in figure 7, where the direction of the stresses is also indicated, and the torsion constant $J = 193.2$ in.^{4}. The torsion constant of the outer shell alone is $J_o = 113.6$ in.^{4}.

II. COMPARISONS BETWEEN CALCULATION AND EXPERIMENT

Tests on box beams.- Figure 8(a) gives the dimensions of three duralumin box beams tested by the U.S. Army Air Corps (reference 6); figure 8(b) gives the dimensions of five stainless steel beams tested by the same agency (reference 7). The test points for any given test run always fell very close to a straight line; individual test curves are therefore not reproduced in the present paper.

The experimental values of the torsional stiffnesses are given in table I, which gives also the torsional stiffnesses calculated by formulas (2) or by equations (5) and (8). The thickness t of the vertical walls of the steel beams was replaced in these calculations by the effective thickness $t_e = \frac{5}{8}\,t$ because these walls formed diagonal-tension fields at low torques. (See reference 8.)

The value of the shear modulus was taken as $G = 4 \times 10^6$ pounds per square inch for duralumin and $G = 10 \times 10^6$ for stainless steel. The shear modulus for stainless steel was taken lower than for ordinary steel in accordance with the facts that the tension modulus of elasticity E for stainless steel is considerably lower than that of ordinary steel and that the shear modulus of other highly alloyed steels has been found to be as low as 8×10^6.

Table I gives next the ratio of experimental stiffness to calculated stiffness. It will be seen that the average ratio of all the beams is 0.90.

In the group of stainless steel beams, beam 4 shows the smallest ratio, which may be attributed to the complicated section of the built-up stiffeners requiring many joints.

Duralumin beam 1 has a ratio considerably in excess of unity. The test reports (references 6 and 7) note that there must have been some test irregularity, because the experimental stiffness of beam 1 was higher than that of beams 2 and 3, which does not seem reasonable.

Possible variations of elastic constants and of sheet thicknesses from the nominal values, however, may together account for perhaps 15 percent of the excess stiffness, which would reduce the experimental stiffness constant practically to the theoretical value. Since no direct error could be found that would make it necessary to eliminate the test result on beam 1, it was included in the average.

A number of tests described in reference 6 and discussed in reference 8 dealt with cases where the stiffness decreases very materially with increase of load. For the present purpose only the initial stiffnesses of those beams come in question, and they are not sufficiently well defined experimentally to give detailed numerical values; inspection of the results indicates that the ratio of experimental to theoretical stiffness lies in general between 0.9 and 1.

It is suggested, therefore, that $\eta = 0.90$ be used as a general factor of effectiveness for box beams in torsion.

Effectiveness of stiffeners.- The outer cover of a shell is more effective in resisting twisting stresses than any material on the inside of the shell. It seemed of some interest, therefore, to calculate for the test beams the torsional stiffness of the outer cover alone, disregarding the stiffeners entirely, and to compare this stiffness GJ_o with the calculated stiffness GJ, which includes the influence of the stiffeners. The stiffness GJ_o, as well as the ratio of GJ to GJ_o is given in table I. Next in the table is listed the reinforcement, expressed by the ratio of the area of the stiffeners to the area of the stiffened sheet. Figure 9 shows the curve of increase in stiffness against reinforcement; it should be remembered that this curve is not generally applicable.

A more logical way to represent the effect of the stiffeners on the torsional stiffness is as follows: Imagine the stiffeners removed; then increase the thickness of the sheet from which the stiffeners have been removed until the torsional stiffness is the same as it was with the stiffeners present. Calculate the amount of material that had to be added to the cover sheets; the ratio of this material to the actual stiffener material gives a measure of the effectiveness of the stiffeners and is listed in the last row of table I. The efficiency of the hat-shape stiffener calculated on this basis is only about 7 percent.

Tests on complete wings.- The experimental wing described in reference 9 was chosen as the first example of a complete duralumin wing. The important characteristics of this wing are shown in figure 10. It consists of a central box with corrugated cover; but a smooth sheet forms a continuous cover over the nose, the central box, and the trailing-edge portion.

The wing was first tested in the elastic range to determine the stiffness. Then it was subjected to the usual static tests, which were carried to destruction in the high-angle-of-attack condition. The break was repaired, and the elastic stiffnesses were determined again in the following three conditions of the wing: (1) complete; (2) after removal of leading edge, leaving the central box and trailing edge; (3) after removal of leading and trailing edges, leaving only the central box.

Figure 11 shows the calculated and experimental results for the box alone. The agreement is very good except at the last station near the tip. Figure 12 shows the results for the combination of box and trailing edge; the calculated curve for the box alone is shown in dotted lines. It is apparent that the effectiveness of the trailing-edge portion is very low, a fact that can be easily explained. The trailing-edge portion buckles into a diagonal-tension field. In order to realize the theoretical stiffness of such a field, rigid flanges must be provided to take up the transverse component of the diagonal tension. The trailing-edge strip, however, is so flexible that it furnishes practically no resistance to these stresses and the cover sheet cannot develop any stiffness. Figure 12 shows that no large error is committed if the trailing-edge portion aft of the rear spar is entirely neglected; this procedure recommends itself also because it reduces very materially the labor of computing the stiffness of the complete wing, a two-cell box requiring very much less computation than a three-cell box. The trailing edge was therefore neglected in calculating the stiffness of the complete wing and figure 13 shows excellent agreement between the calculated and the experimental twist.

A point that deserves some mention is the calculation of the effective thickness of the webs. These webs had triangular lightening holes, making the webs, in effect, trusses with double diagonals. The effective thickness of these webs was calculated by formula (11) of reference 10. This formula is valid for pin-jointed trusses; the trusses in question here have rigid joints, and the effect of these joints was taken into account by multiplying the calculated effective thickness by a factor 1.20 based on calculations and tests on similar trussed webs given in reference 3.

Farther outboard, the webs had circular lightening holes. The effect of these holes on the shear stiffness of the webs was estimated from tests (reference 11).

As the second example of a complete duralumin wing, the wing shown in figure 14 was chosen. It has a central two-cell box covered with smooth sheet stiffened by closed-section stiffeners. The leading and trailing edges are fastened to the central box by means of piano hinges leaving them virtually open sections ineffective in torsion, at least at low loads. The torsionally effective part of the wing is indicated by the full lines in the plan and by the crosshatching in the sections.

The interesting feature of this wing with respect to calculating the torsional stiffness is the large well for the retracting wheel. Obviously, only the box between the center and rear webs is effective between ribs 1 and 3. At rib 5, the full section from front web to rear web is effective. Between ribs 3 and 5, the front part of the box is cut up to form the recesses for the landing-gear struts. No detail drawings on which an estimate of the efficiency could be based were available for this portion; it was assumed, therefore, that the torsional stiffness varied linearly between ribs 3 and 5.

The cut-out being close to the root, the loss in torsional stiffness of the shell is partly balanced by the bending stiffness of the spars. The twist at rib 4 was therefore calculated by formula (10a) of reference 10, using weighted averages of moments of inertia and torsional stiffness between the root fittings and rib 4. It is obviously not possible to calculate the curve of twist between the root and rib 4, but this lack is of no practical importance.

The test load was applied in four increments; the test points plotted in figure 15 are the averages of the four sets of readings. The outboard part of the shell buckled about in the middle of the test range; calculations were therefore made for the nonbuckled state as well as for the buckled state. The agreement between experiment and calculation is good in the outboard part; inboard there is a rather large percentage error, but this error is not large in absolute magnitude; it may be partly due to jig deflection.

<u>Stiffness under large torques</u>.- The theoretical formulas discussed give the initial torsional stiffness under very low torques. For torques in the practical working range it will very often be necessary to apply corrections. One type of correction has been mentioned and used in the text: If the smooth cover buckles to form a diagonal tension field, the actual sheet thickness t must be replaced by the effective thickness $t_e = \frac{5}{8} t$. This effective thickness may be decreased much further at high loads (reference 8). Corrugated or well-stiffened sheet can probably be assumed to lose not more than 5 or 10 percent of its stiffness until failure occurs although there is no direct experimental evidence available to substantiate this claim.

It is apparent, then, that it is necessary before starting a stiffness calculation to define the load range in which it is to apply and to make corresponding corrections if necessary to the formulas for initial stiffness.

Langley Memorial Aeronautical Laboratory,
National Advisory Committee for Aeronautics,
Langley Field, Va., July 16, 1935.

REFERENCES

1. Timoshenko, S.: Strength of Materials, Part II. D. Van Nostrand Co., Inc., 1930.

2. Atkin, E. H.: Torsion in Thin Cylinders. Flight - The Aircraft Engineer, Sept. 25, 1931, pp. 70-72, and Oct. 30, 1931, pp. 76-77.

3. Hertel, Heinrich: Die Verdrehsteifigkeit und Verdrehfestigkeit von Flugzeugbauteilen. D.V.L. Jahrbuch, 1931, S. 165-220.

4. Van der Neut, A.: Twisting and Bending by End Load of Multiply Connected Box Spars. Verslagen en Verhandelingen van den Rijks-Studiedienst voor de Luchtvaart, Amsterdam, Deel VI, 1931, p. 67. (Dutch text, English summary.)

5. Duncan, W. J.: The torsion and Flexure of Cylinders and Tubes. R. & M. No. 1444, British A.R.C., 1932.

6. Greene, C. F., and Younger, J. E.: Metal Wing Construction. Part I - Experimental Studies and Discussion. A.C.T.R., Serial No. 3361, Matériel Division, Army Air Corps, 1929.

   Carpenter, S. R.: Metal Wing Construction. Part III - Compilation of Test Data. A.C.T.R., Serial No. 3333, Matériel Division, Army Air Corps, 1930.

7. Brown, C. G., and Schwartz, E. H.: Metal Wing Construction. Part IV - Spot-Welded Stainless Steel Box Beams. A.C.T.R., Serial No. 3900, Matériel Division, Army Air Corps, 1933.

8. Kuhn, Paul: The Torsional Stiffness of Thin Duralumin Shells Subjected to Large Torques. T.N. No. 500, N.A.C.A., 1934.

9. Brown, C. G., and Greene, C. F.: Static-Test and Stress-Distribution Studies of the Matériel Division 55-Foot Cantilever All-Metal Wing. A.C.I.C. No. 663, Matériel Division, Army Air Corps, 1932.

10. Kuhn, Paul: Analysis of 2-Spar Wings with Special Reference to Torsion and Load Transference. T.R. No. 508, N.A.C.A., 1935.

11. Mathar, J.: Beitrag zur Schubsteifigkeit und Knickfestigkeit von gelochten dunnen Platten. Abhandlungen aus dem Aero. Inst. der Technischen Hochschule, Aachen, Heft 10, 1931.

TABLE I

Experimental and Calculated Torsional Stiffnesses

	Duralumin beams			Stainless steel beams				
Number of beam:	1	2	3	4	5	6	7	8
Experimental stiffness GJ (10^6 lb.-in.^{2})	45.1	41.5	43.2	20.2	23.9	29.8	30.6	20.2
Calculated stiffness GJ	38.5	53.8	55.5*	25.6	25.4	30.2	32.7	23.5
Ratio of experimental to calculated stiffness	1.171	.772	.778	.790	.940	.987	.935	.860
Average ratio (η)	.907			.901				
Stiffness GJ_o disregarding stiffeners		23.2		18.49	17.4	28.1	32.3	20.9
Ratio of GJ_o to calculated GJ		2.32		1.38	1.46	1.08	1.01	1.13
Ratio of stiffener cross-sectional area to area of cover sheet		4.10		2.51	2.52	.53	.52	2.24
Effectiveness factor for stiffeners (see text)		0.41		.27	.37	.37	.06	.09

Duralumin: $G = 4 \times 10^6$ lb. per sq.in. Max. torque: $T = 5000$ in.-lb. for beams 1 to 3
Stainless steel: $G = 10 \times 10^6$ lb. per sq.in. $T = 4000$ in.-lb. for beams 4 to 8.

*By approximate method.

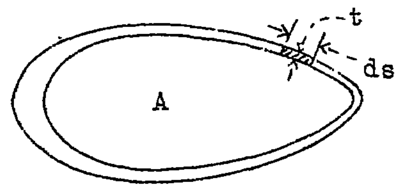

Figure 1.- Simple torsion tube.

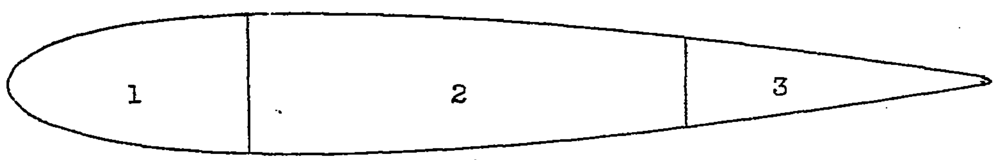

Figure 2.- Shell with interior webs.

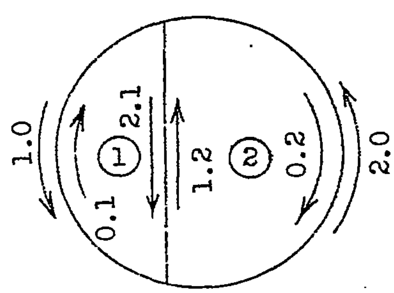

Figure 3.- Diagram for notation.

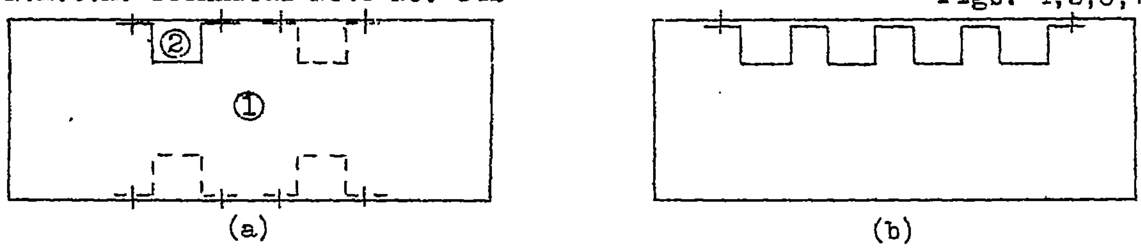

Figure 4.- Box beam with stiffeners.

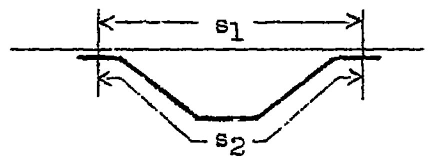

Figure 5.- Stiffener section.

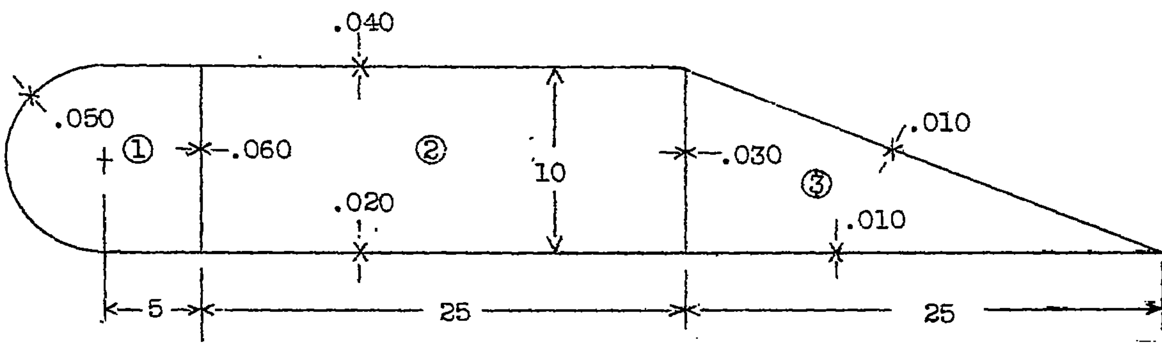

Figure 6.- Schematic profile.

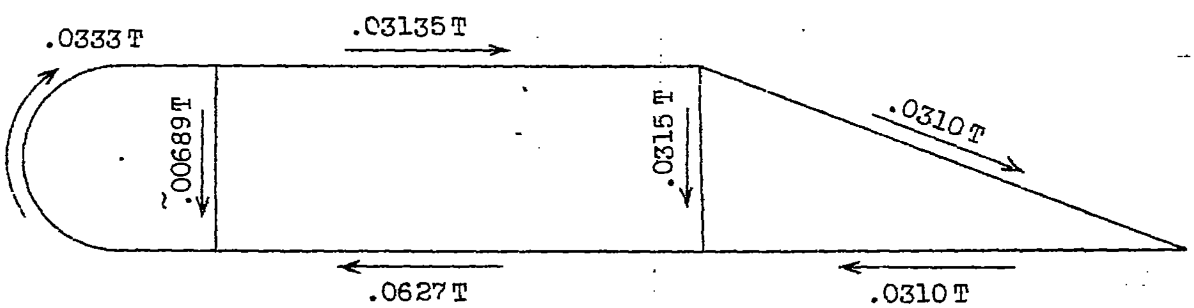

Figure 7.- Stress sheet for schematic profile.

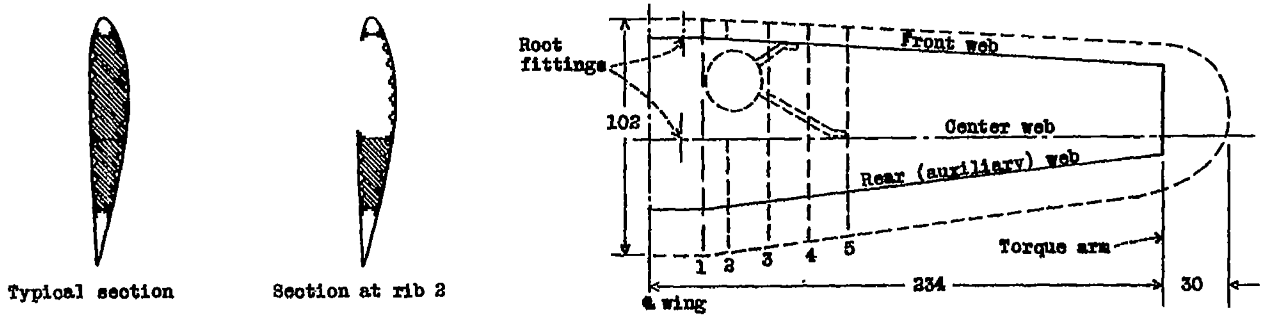

Figure 14.- Wing with wheel cut-out.

All beams symmetrical about center line.

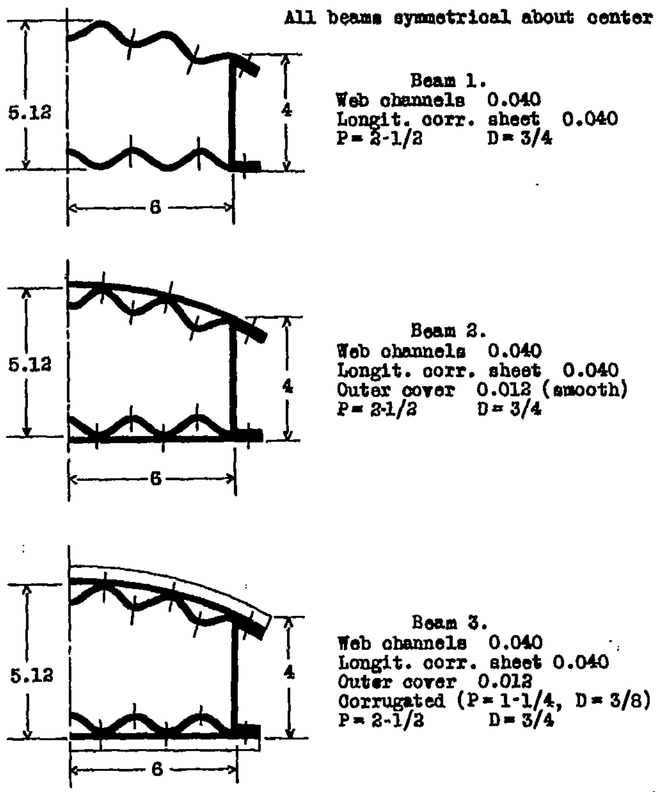

Figure 8(a).- Duralumin box beams.(1-3)

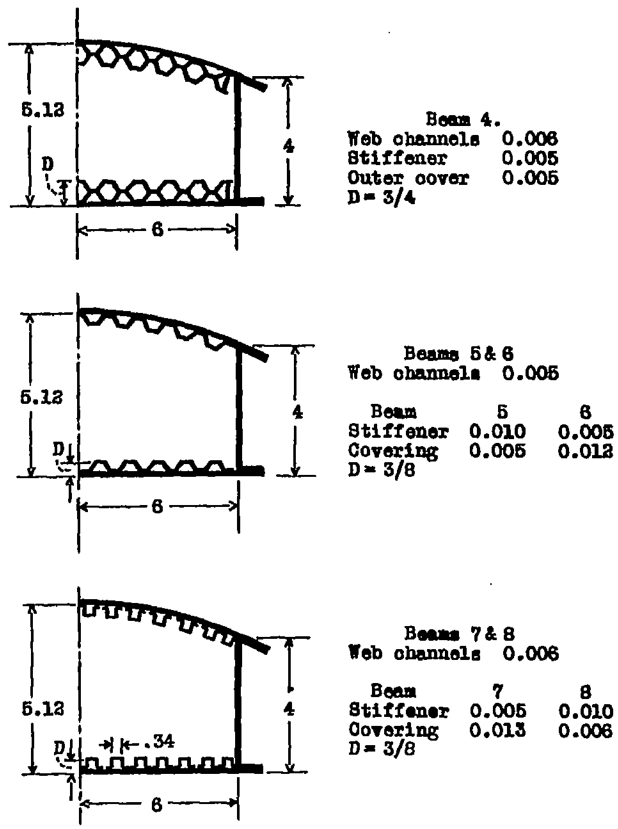

Figure 8(b).- Stainless steel box beams.(4-8)

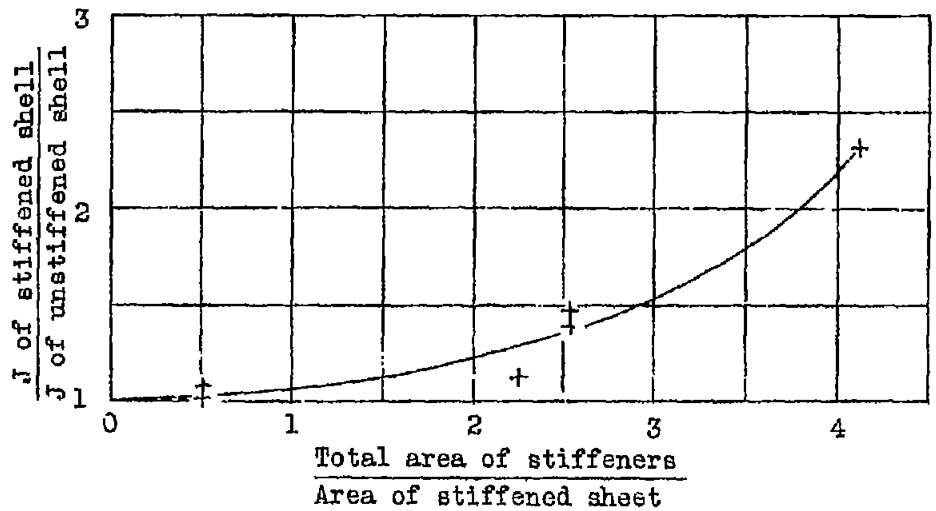

Figure 9.- Influence of stiffeners on torsional stiffness.

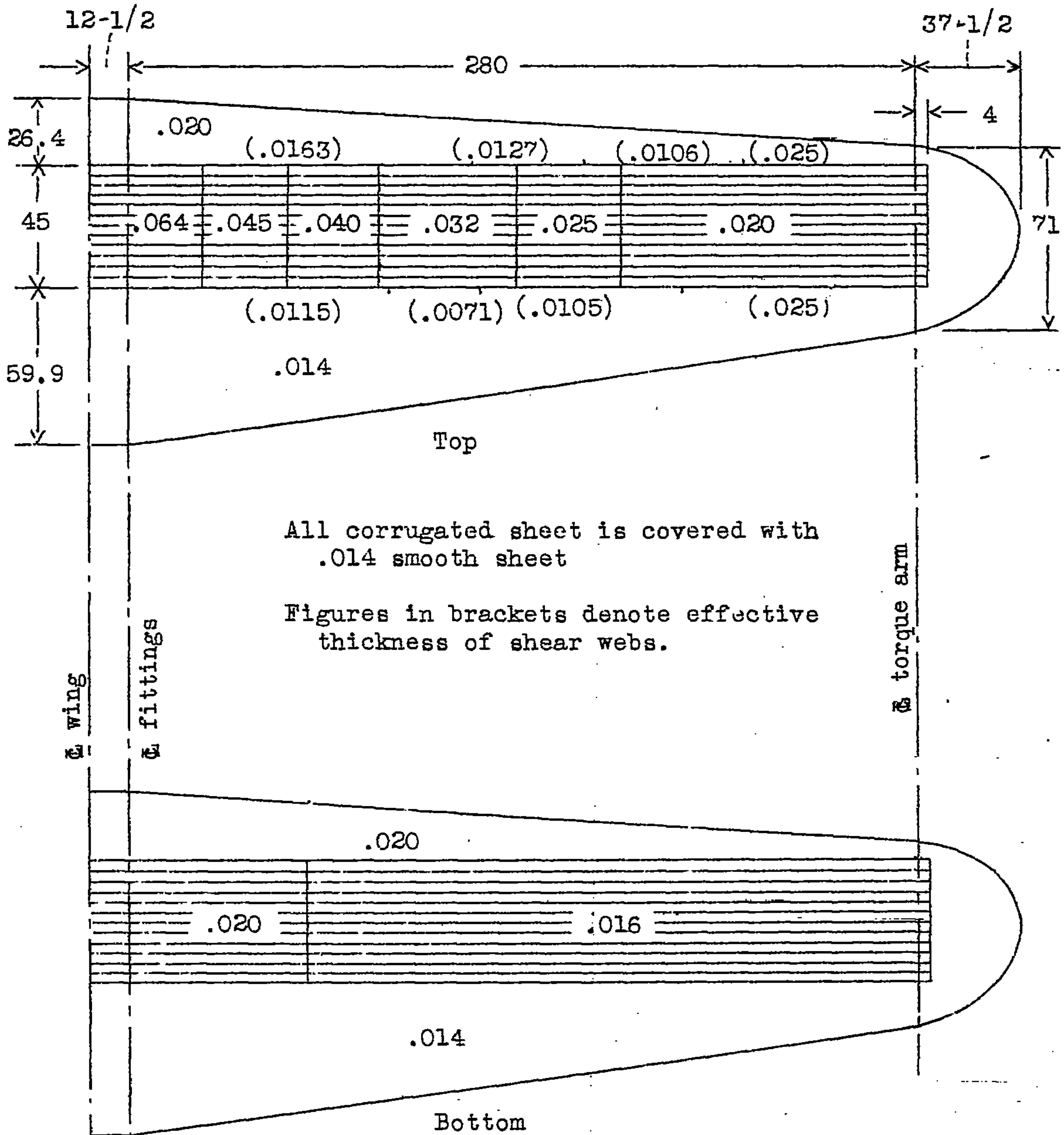

Airfoil: U.S.A. 35 model
Root thickness: 21.8%
Tip thickness: 13.5%

Figure 10.- Matériel Division 55-foot wing.

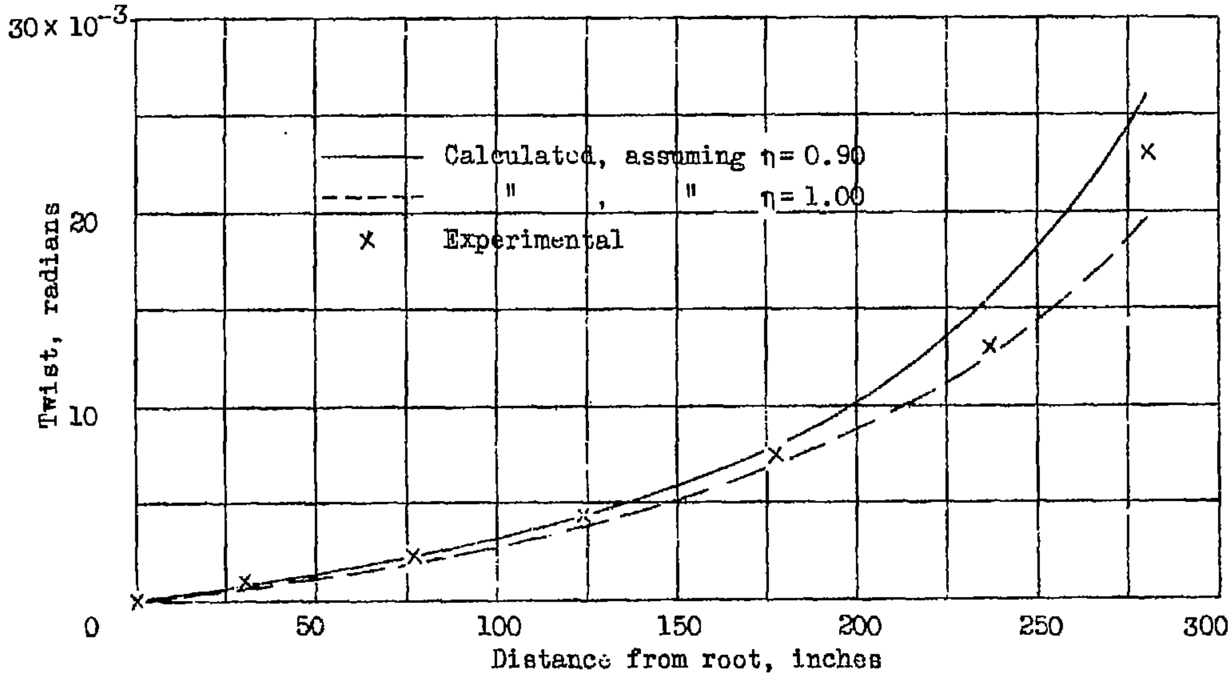

Figure 11.- Twist of box alone.

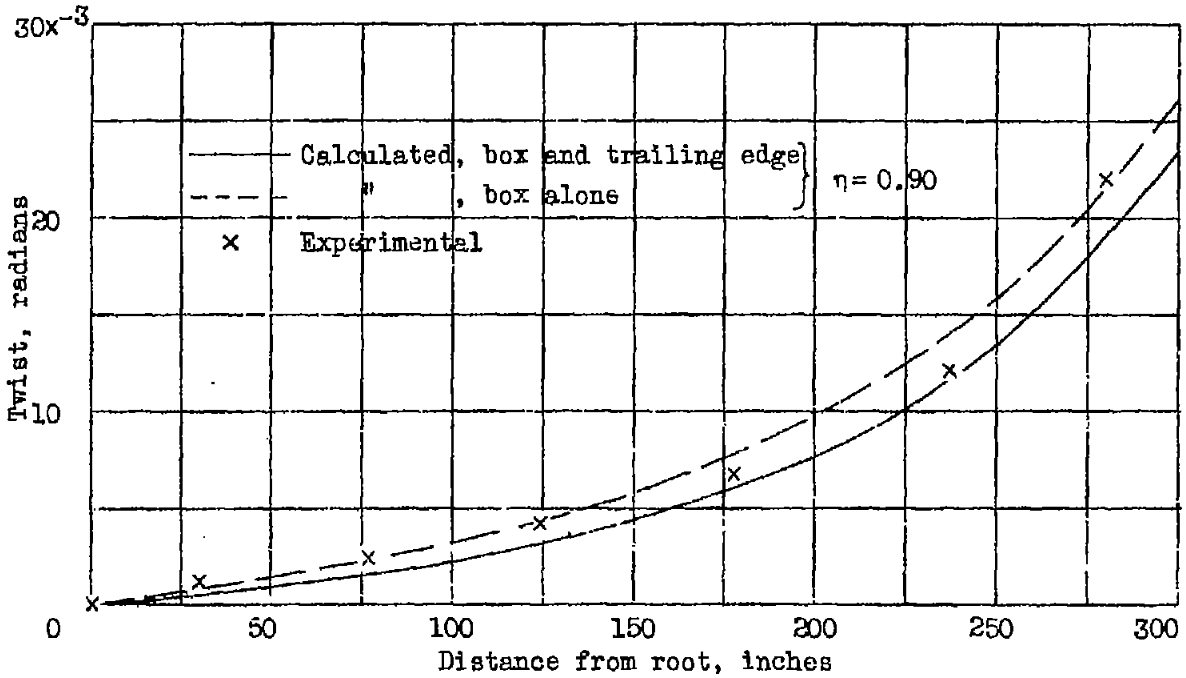

Figure 12.- Twist of combination box and trailing edge.

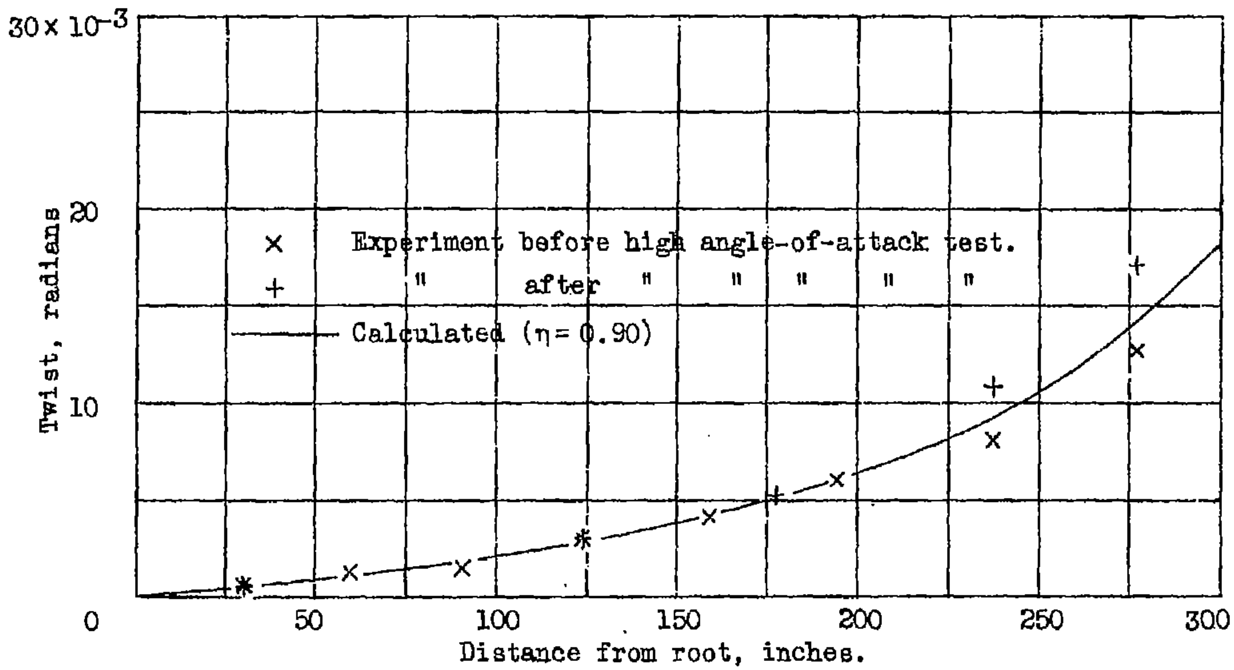

Figure 13.- Twist of complete wing.

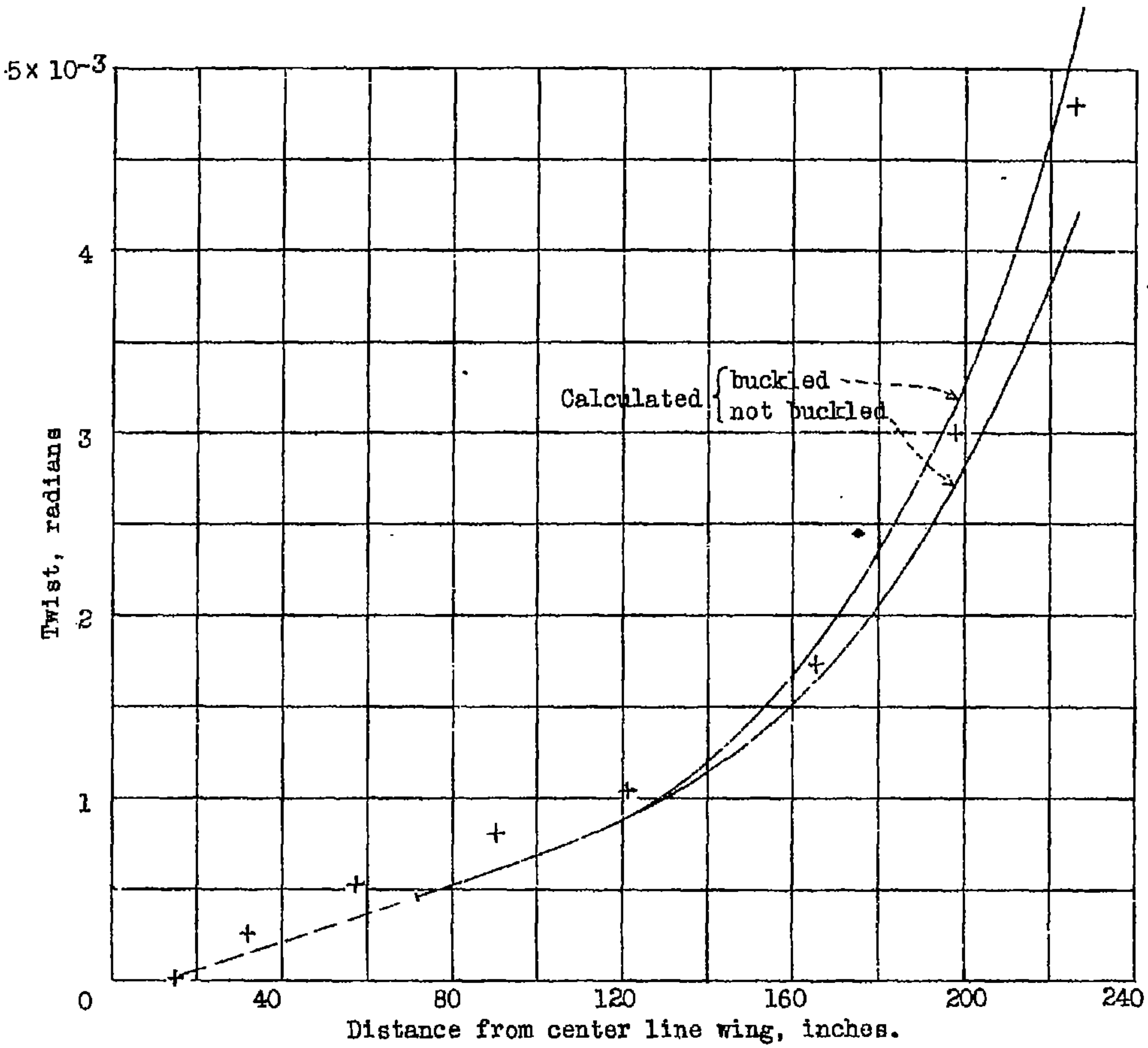

Figure 15.- Twist of wing shown in figure 14.